

## Effect of a magnetic field on Mott-Hubbard systems

Laurent Laloux\* and Antoine Georges†

*Laboratoire de Physique Théorique de l'Ecole Normale Supérieure, 24, rue Lhomond, 75231 Paris Cedex 05, France*

Werner Krauth‡

*Laboratoire de Physique Statistique de l'Ecole Normale Supérieure, 24, rue Lhomond, 75231 Paris Cedex 05, France*

(Received 3 March 1994)

The effect of a magnetic field on Mott-Hubbard systems is investigated by studying the half-filled Hubbard model in the limit of infinite dimensions. A first-order metamagnetic transition between the strongly correlated metal and the Mott insulator is found for a critical value of the applied field. The field and temperature dependence of the magnetization, one-particle properties, and susceptibility are studied and compared to the Gutzwiller approximation. The experimental relevance for transition-metal oxides and liquid  $^3\text{He}$  is discussed.

### I. INTRODUCTION

Systems that are close to a Mott-Hubbard transition between a paramagnetic metal and a paramagnetic insulator display local magnetic moments interacting through a residual antiferromagnetic exchange. Hence, the response of such systems to a magnetic field is an interesting physical problem in which a competition takes place between the exchange and the alignment of the local moments with the external field. On the metallic side of the transition, the problem is even more involved, since an additional energy scale exists (the local Kondo temperature, or effective Fermi energy), associated with the quenching of local spin fluctuations at low temperature.

Up to now, the only available quantitative description of this problem has been the Gutzwiller approximation.<sup>1-4</sup> The susceptibility of the strongly correlated metal is predicted to increase with the field in this approach, and a first-order localization transition (metamagnetic transition) is found for a critical value of the applied field.<sup>3,4</sup> The Gutzwiller approximation has limitations, however. The main one is that it neglects the residual exchange altogether, so that it cannot account for the physics of the above competition. The Mott insulator is caricatured as a collection of independent local moments, which has infinite susceptibility at zero temperature, and the susceptibility also diverges as the metal-insulator transition is reached from the metallic side. Finally, this approximation is restricted to zero temperature (although some finite-temperature extensions have been attempted<sup>4-6</sup>).

Recently, an approach to the Mott transition has been proposed<sup>7,8</sup> and extensively studied,<sup>9-13</sup> based on the Hubbard model in the controlled limit of infinite spatial dimensionality ( $d \rightarrow \infty$ ).<sup>14-16</sup> The exchange is (at least partially) taken into account in this limit, and finite temperature effects can be addressed in a consistent manner. The aim of the present paper is to study the effect of a magnetic field on the Mott transition (as well as on the correlated metal or deep into the insulator) within

this approach. Some earlier attempts have appeared in the literature,<sup>9,11,17</sup> but have not been able to solve the problem in the low-temperature or low magnetic-field regime because of limitations in the numerical method employed. We find that at very low temperature a magnetic field does drive the strongly correlated metal closer to localization and that a first-order metamagnetic transition to the Mott insulator takes place for a critical value of the applied field. This is our main new result, which is in qualitative agreement with the predictions of the Gutzwiller approximation (even though the magnetic exchange significantly modifies the quantitative results of this approximation). We establish that, near this transition and at finite temperature, the magnetic susceptibility is an *increasing* function of the magnetic field. We also provide further evidence that the zero-field Mott transition is first order at finite temperature and show that the magnetic properties of both the weakly correlated metal and the Mott insulating phase can be understood quantitatively in a simple manner.

There are several experimental motivations to our work. It has been demonstrated in previous studies<sup>9,11</sup> that the  $d = \infty$  approach to the Mott transition agrees qualitatively (and, for some properties, quantitatively) with many observed features of the paramagnetic-metal-paramagnetic-insulator transition of transition-metal oxides. There have been some investigations of magnetic properties close to this transition [e.g., for  $(V_{1-x}Cr_x)_2O_3$  in Ref. 18], with which our results are in satisfactory qualitative agreement. The recent experiments on the field dependence of the magnetization of liquid  $^3\text{He}$  (Ref. 19) provide another important motivation. There are two competing descriptions of this strongly correlated Fermi liquid. The Stoner and paramagnon approach<sup>20</sup> views the system as close to a ferromagnetic transition, while the “almost localized” approach<sup>21,3</sup> views it as a strongly correlated liquid close to Mott localization and relies on a Hubbard model lattice description. Quantitative predictions in the latter approach have up to now relied on the use of the Gutzwiller approximation.<sup>3</sup> These

two approaches have led to very different predictions for the response to an external field: the Stoner approach predicts a smooth magnetization ( $\partial\chi/\partial h < 0$ ), while the Gutzwiller approximation exhibits a first-order metamagnetic transition, with  $\partial\chi/\partial h > 0$  close to the transition. One of the main purposes of the above experiments has been to discriminate between them. Our results on a well-controlled limit of a specific model provide a test of both approximation schemes and confirm that a description of liquid  $^3\text{He}$  by a lattice Hubbard model rigidly maintained at half filling is inappropriate.

This paper is organized as follows. In Sec. II we define the model, explain the numerical methods and briefly summarize previously established results on the zero-field Mott transition in the  $d = \infty$  limit. In Sec. III, we give an overview of our numerical results for the field dependence of the magnetization and of the phase diagram as a function of field and temperature. In Sec. IV, some aspects of the Gutzwiller approximation for the model under study are summarized. Section V is devoted to a detailed description and discussion of our results, and Sec. VI to some comparisons with experiments and concluding remarks.

## II. MODEL, METHODS, AND ZERO-FIELD MOTT TRANSITION

### A. The Hubbard model in infinite dimensions

We consider in this paper the Hubbard model in a uniform magnetic field at half filling ( $\mu = U/2$ ):

$$H = - \sum_{(ij),\sigma} (t_{ij} c_{i\sigma}^{\dagger} c_{j\sigma} + \text{H.c.}) + U \sum_i n_{i\uparrow} n_{i\downarrow} - \sum_{i\sigma} (\mu + h\sigma) n_{i\sigma} \quad (1)$$

with nearest-neighbor hopping on a lattice of connectivity  $z$ , in the limit  $z \rightarrow \infty$ . The hopping must be scaled<sup>14</sup> as  $t_{ij} = t/\sqrt{2z}$  to keep the problem nontrivial in this limit. For simplicity, we consider in the following a Bethe lattice, for which the free ( $U = 0$ ) density of states (DOS)  $D(\epsilon) = \sum_{\mathbf{k}} \delta(\epsilon - \epsilon_{\mathbf{k}})$  takes a semicircular form in the limit  $z \rightarrow \infty$ :  $D(\epsilon) = \frac{1}{\pi t} \sqrt{2 - (\epsilon/t)^2}$ . Unless explicitly stated, we set  $t = 1$  in the following.

Following Ref. 15 (cf. also Refs. 22 and 23), all the local properties of the model can be obtained *via* a single-site impurity problem supplemented by a self-consistency condition. The effective action of this impurity problem, in the presence of a magnetic field, reads

$$S = - \int_0^{\beta} d\tau \int_0^{\beta} d\tau' \sum_{\sigma} c_{\sigma}^{\dagger}(\tau) [G_{0\sigma}^{-1}(\tau - \tau')] c_{\sigma}(\tau') + U \int_0^{\beta} d\tau n_{\uparrow}(\tau) n_{\downarrow}(\tau), \quad (2)$$

where, in the *paramagnetic phase*, the “bare” Green’s function  $G_{0\sigma}$  is related to the interacting Green’s func-

tion  $G_{\sigma}(\tau - \tau') \equiv -\langle T c(\tau) c^{\dagger}(\tau') \rangle_{\mathcal{S}}$  through a self-consistency equation. For the Bethe lattice, it reads

$$G_{0\sigma}^{-1}(i\omega_n) = i\omega_n + \mu + h\sigma - \frac{t^2}{2} G_{\sigma}(i\omega_n). \quad (3)$$

The self-energy of the lattice model reads  $\Sigma_{\sigma}(i\omega_n) = G_{0\sigma}^{-1}(i\omega_n) - G_{\sigma}^{-1}(i\omega_n)$  and is independent of momentum<sup>24</sup> in the  $z \rightarrow \infty$  limit. Because of the magnetic field, these equations depend on spin, but at half filling ( $\mu = U/2$ ), the symmetry property  $F_{\sigma}(-i\omega_n) = -F_{-\sigma}(i\omega_n)$  holds, where  $F$  is any of the functions  $G_{\sigma}$ ,  $G_{0\sigma} - \mu$ , or  $\Sigma_{\sigma} - \mu$ .

It is useful<sup>15</sup> to view the effective action  $S$  as that of an Anderson model with a spin-dependent hybridization function  $\Delta_{\sigma}(\omega)$ , where the conduction-electron “bath” has been integrated out:

$$G_{0\sigma}^{-1}(i\omega_n) = i\omega_n + \mu + h\sigma - \int_{-\infty}^{+\infty} d\omega \frac{\Delta_{\sigma}(\omega)}{i\omega_n - \omega}. \quad (4)$$

For the Bethe lattice, the self-consistency condition (3) specifies the hybridization function in terms of the interacting local spectral density  $\rho_{\sigma}(\omega) \equiv -\frac{1}{\pi} \text{Im} G_{\sigma}(\omega + i0^+)$  through  $\Delta_{\sigma}(\omega) = \frac{t^2}{2} \rho_{\sigma}(\omega)$ . Although highly simplified, this coupled problem remains unsolvable analytically: numerical methods are necessary to obtain a full solution.

In this work, we follow the *paramagnetic* solutions of these coupled equations, even though the model actually has a transition to an antiferromagnetic phase below some Néel temperature for arbitrary  $U$  (the Bethe lattice is a bipartite lattice). This is possible, since  $z \rightarrow \infty$  is a mean-field limit in which the continuation of a solution of the mean-field equations in an unstable region has a well-defined mathematical meaning. Alternatively, one may wish to consider a model that does not display antiferromagnetic ordering and for which the solutions studied in this paper describe the actual ground state. As discussed in Refs. 25, 9, and 11, an example of such a model is a Hubbard model on a *fully connected* cluster of  $N$  sites, with randomness on the hopping parameters  $t_{ij}$ :

$$H = - \sum_{\sigma; i, j=1}^N t_{ij} c_{i\sigma}^{\dagger} c_{j\sigma} + U \sum_i n_{i\uparrow} n_{i\downarrow} \quad \text{with } \overline{t_{ij}^2} = \frac{t^2}{2N}. \quad (5)$$

It can be shown that the single-particle Green’s function of this random model coincides with the same quantity for the *paramagnetic phase* of the Hubbard model on the  $z = \infty$  Bethe lattice, with no randomness and hopping parameter  $t_{ij} = t/\sqrt{2z}$ . It is clear, however, that the phase diagram of the two models differ: the disordered one has a highly degenerate singlet ground state for large  $U$  at half filling and *no antiferromagnetic phase*.

### B. Numerical method: exact diagonalization for a fixed magnetization

For a given value of the interaction strength and temperature, and a given magnetic field  $h$ , the above set of

coupled equations can be solved following the usual two-step procedure: (i) calculation of  $G_{\uparrow}, G_{\downarrow}$  for a given pair of  $G_{0\uparrow}, G_{0\downarrow}$  and (ii) calculation of  $G_{0\uparrow}^{\text{new}}, G_{0\downarrow}^{\text{new}}$  using the self-consistency relation. Step (i) involves the solution of the Anderson model with a given conduction bath. This can be achieved by two possible algorithms: the quantum Monte Carlo Hirsch-Fye algorithm, used in this context in Refs. 16, 7, and 8, and the exact diagonalization method.<sup>26</sup> As shown in previous work, the exact diagonalization method is far more efficient for the problem at hand than the quantum Monte Carlo method, against which it has been carefully checked, and we shall use it in the present work. Step (ii) updates the conduction bath self-consistently. An iteration of this procedure indeed converges for not too small magnetic fields that are not too close to the metal-insulator transition. In order to investigate these ranges of parameters, a modification of this procedure must be used,<sup>27</sup> which seeks convergence for a *fixed* value of the *magnetization*, as described below. This is the main technical point that allows us to obtain the results described here.

The continuous conduction-electron bath is parametrized by a finite number of parameters  $(\{\epsilon_{k\sigma}, V_{k\sigma}\})$ ,  $k = (2, \dots, n_s), \sigma = \uparrow, \downarrow$ . The Hamiltonian of the corresponding Anderson model reads

$$H_{\text{And}} = \sum_{\sigma} \epsilon_{d\sigma} d_{\sigma}^{\dagger} d_{\sigma} + \sum_{\sigma, k=2}^{n_s} \epsilon_{k\sigma} a_{k\sigma}^{\dagger} a_{k\sigma} + U n_{d\uparrow} n_{d\downarrow} + \sum_{\sigma, k=2}^{n_s} (V_{k\sigma} a_{k\sigma}^{\dagger} d_{\sigma} + \text{H.c.}). \quad (6)$$

The Green's function  $G_{0\sigma}$  of the impurity site  $d_{\sigma}$  is then represented by

$$G_{0\sigma}^{\text{And}} = \left( i\omega_n - \epsilon_{d\sigma} - \sum_{k=2}^{n_s} \frac{V_{k\sigma}^2}{i\omega_n - \epsilon_{k\sigma}} \right)^{-1}, \quad (7)$$

where  $i\omega_n = (2n+1)\pi/\beta$  and with the symmetries at half filling:

$$\begin{cases} \epsilon_{d\sigma} = -(U/2 + h\sigma) \\ \epsilon_{k\downarrow} = -\epsilon_{k\uparrow} \\ V_{k\downarrow}^2 = V_{k\uparrow}^2 \end{cases} \quad (8)$$

An exact diagonalization of  $H_{\text{And}}$  is performed to obtain the Green's function  $G_{\sigma}$ , and a function  $G_{0\sigma}^{\text{new}}$  is deduced from the self-consistency condition. Then, the new Green's function  $G_{0\sigma}^{\text{And new}}$  is calculated. This is done by minimizing with respect to  $\{\epsilon_{k\sigma}^{\text{new}}, V_{k\sigma}^{\text{new}}\}$  the following cost function, *on the imaginary axis*,

$$\chi^2 = \frac{1}{n_{\text{max}} + 1} \sum_{n=0}^{n_{\text{max}}} |G_{0\sigma}^{-1\text{new}}(i\omega_n) - G_{0\sigma}^{-1\text{And new}}(i\omega_n)|. \quad (9)$$

In practice, a conjugate gradient method is used to perform the minimization. On a workstation, complete diagonalization of the Hamiltonian is possible for  $n_s \leq 6$  at all temperatures, and the Lanczòs algorithm allows

us to calculate directly zero-temperature properties up to  $n_s \sim 10$ . At zero temperature,  $\beta$  is used as a fictitious temperature serving as a cutoff at small frequencies. The difference between  $G_{0\sigma}$  and  $G_{0\sigma}^{\text{And}}$  provides a test of the accuracy of the method (which is exact in the limit  $n_s \rightarrow \infty$ ). In practice, a good accuracy is obtained already for  $n_s = 4$  for a temperature as low as  $\beta \simeq 100$ .

We now describe in more detail the precise algorithm used at a *fixed value of the magnetization*.

(i) For a given set  $\{\epsilon_{k\sigma}, V_{k\sigma}\}$ , we find the magnetic field  $h = -\mu - \epsilon_{d\uparrow}$ , which gives the desired magnetization  $m$ . Then we calculate the Green's functions  $G_{\sigma}$  and  $G_{0\sigma}^{\text{new}}$  for this field  $h$ .

(ii) The new set  $\{\epsilon_{k\sigma}^{\text{new}}, V_{k\sigma}^{\text{new}}\}$  is obtained from  $G_{0\sigma}^{\text{new}}$  with the  $\chi^2$  fit.

The convergence is obtained for a fixed value of the interaction  $U$  and the magnetization  $m$ , when both  $\{\epsilon_{k\sigma}, V_{k\sigma}\}$  and  $h$  are stabilized.

Using the above method, we are interested in computing the following physical quantities: *uniform magnetization*, defined as

$$m = \langle n_{\uparrow} - n_{\downarrow} \rangle = G_{\uparrow}(\tau = 0^-) - G_{\downarrow}(\tau = 0^-), \quad (10)$$

*uniform susceptibility*  $\chi$ , calculated by numerical differentiation,

$$\chi = \frac{m(h + \Delta h) - m(h)}{\Delta h}, \quad \Delta h \rightarrow 0 \quad (11)$$

(note that the susceptibility can also be calculated from an evaluation of a two-particle Green's function for the impurity model<sup>28,16</sup>), *local susceptibility*  $\chi_{\text{loc}}$  is the response of the system to a local magnetic field applied *on a single site* (taken as the impurity site),

$$\begin{aligned} \chi_{\text{loc}} &= \int_0^{\beta} d\tau \langle T \{ [n_{\uparrow}(0) - n_{\downarrow}(0)] - m \} \\ &\quad \times \{ [(n_{\uparrow}(\tau) - n_{\downarrow}(\tau)) - m] \} \rangle \\ &= \sum_{\alpha, \gamma} \frac{|\langle \alpha | S_z - m | \gamma \rangle|^2}{E_{\gamma} - E_{\alpha}} (e^{-\beta E_{\alpha}} - e^{-\beta E_{\gamma}}), \end{aligned} \quad (12)$$

and the *local density of states*  $\rho_{\sigma}(\omega) = -\frac{1}{\pi} \text{Im} G_{\sigma}(\omega + i0^+)$  can be computed from the spectrum and matrix elements. For finite  $n_s$ , it is a sum of  $\delta$  functions, which nevertheless give a satisfactory account of the main spectral features.

### C. The Mott transition in zero field

We briefly summarize in this section the understanding of the Mott transition for zero external field that has been reached in previous work<sup>7-13</sup> and that is further extended by the present study. The coupled equations (2) and (3) for the zero-field Green's function have two types of solutions at zero temperature. Metallic solutions have the characteristic low-frequency behavior of a Fermi liquid:<sup>29</sup>  $\text{Re}\Sigma(\omega + i0^+) = U/2 + (1 - 1/Z)\omega + \dots$ ,  $\text{Im}\Sigma(\omega + i0^+) = -\Gamma\omega^2 + \dots$ .  $Z$  is the quasiparticle residue, which is related here to the effective mass by

$m^*/m = 1/Z$ .<sup>24</sup> A plot of  $Z$  as a function of  $U$  is given in the inset of Fig. 1. In contrast, insulating solutions have  $\text{Re}\Sigma(\omega + i0^+) = C/\omega + \dots$  at low frequencies, while  $\text{Im}\Sigma$  and  $\rho(\omega)$  vanish [except for a  $\delta(\omega)$  piece in  $\text{Im}\Sigma$ ] inside a finite frequency range  $[-\Delta_g/2, \Delta_g/2]$ .  $\Delta_g$  is the Mott gap to charge excitations, and the effective mass is infinite ( $Z = 0$ ).

In the metal, a local moment exists at high temperature (with the local susceptibility  $\chi_{\text{loc}}$  following Curie's law) but is quenched at low temperature, so that  $\chi_{\text{loc}}$  is finite at  $T = 0$ . This quenching is associated with the Kondo effect of the associated impurity model, since for metallic solutions the conduction-electron bath has a finite density of states at the Fermi level [ $\rho(0) \neq 0$ ]. The spin-fluctuation energy scale corresponding to this quenching is the local Kondo temperature  $T_K$ , of the order of  $Zt$ . The conduction-electron bath DOS of insulating solutions has zero spectral weight at low frequency, so that the Kondo effect does not take place and an unquenched local moment exists down to zero temperature. As a result  $\chi_{\text{loc}}$  follows Curie's law and diverges at  $T = 0$ .

A plot of the local susceptibility  $\chi_{\text{loc}}$  vs interaction strength is displayed in Fig. 1 for a finite but low temperature  $T = 0.01$ . It is immediately apparent on this plot that a regime of *coexisting solutions* exists for  $U_{c1}(T) < U < U_{c2}(T)$  and thus that the Mott transition is a *first-order transition* at finite temperature (as in a liquid-gas system), as previously suggested in Refs. 9 and 11. (The study of the coexistence interval with  $n_s=3,4,5,6$  gives the *stabilized* values,  $U_{c1} \simeq 3.3$  and  $U_{c2} \simeq 3.8$  at  $T = 0.01$ ). At finite temperature entropic effects strongly favor the "insulator" (which has a ground-state entropy  $N \ln 2$  in this model) and the first-order transition line must therefore be close to  $U_{c1}(T)$ .

At zero temperature, a locally stable metallic solution

exists for  $U < U_{c2}(0)$ , while an insulating solution is found for  $U > U_{c1}(0)$ . Whether  $U_{c2}(0)$  is actually different from  $U_{c1}(0)$  has not yet been entirely clarified. Evidence that  $U_{c1}(0) \simeq U_{c2}(0)$  has been provided by the Lanczòs results of Ref. 26. Another recent study<sup>12</sup> concludes that  $U_{c1} < U_{c2}$ , and that the  $T = h = 0$  transition is second order at  $U_{c2}(0)$ , for reasons of energetics. These critical points are *a priori* associated with quite different physical phenomena, however.  $U_{c2}(0)$  is a second-order critical point<sup>10,13</sup> at which  $m^*/m$ ,  $\chi_{\text{loc}}$  and the inverse compressibility diverge, much as in the Brinkman-Rice scenario.<sup>2</sup> This reflects the continuous disappearance of coherent low-energy excitations (quasiparticles) in this almost localized Fermi liquid. On the other hand, the disappearance of the insulating solution as  $U$  is lowered below  $U_{c1}(0)$  occurs when the gapped conduction-electron bath can no longer sustain an unquenched local moment. Whether this happens abruptly or with a gap closing continuously at  $U_{c1}(0)$  has not yet been settled in this model.

The response of these phases to a small magnetic field has been discussed in previous work (cf. Refs. 9 and 11). The inset of Fig. 1 displays numerical results for the uniform magnetic susceptibility  $\chi$  as a function of  $U$ , obtained at  $\beta = 100$ .  $\chi$  is finite down to  $T = 0$  in both phases and *does not diverge* as  $U_{c2}(0)$  is approached within the metallic solution, in contrast to  $\chi_{\text{loc}}$ . The reason is that the energy scale for residual antiferromagnetic exchange entering *local* response functions [such as  $\chi_{\text{loc}} = \sum_q \chi(q)$ ] is the exchange between two *fixed* sites  $J_{ij} = t_{ij}^2/U = O(1/d)$ , while the scale entering uniform response functions [such as  $\chi = \chi(q = 0)$ ] is the sum of  $J_{ij}$  over all neighbors:  $J = t^2/2U$ . Hence the former scale disappears from the physics as  $d \rightarrow \infty$ , while the latter remains  $O(1)$ : the exchange is not treated on equal foot-

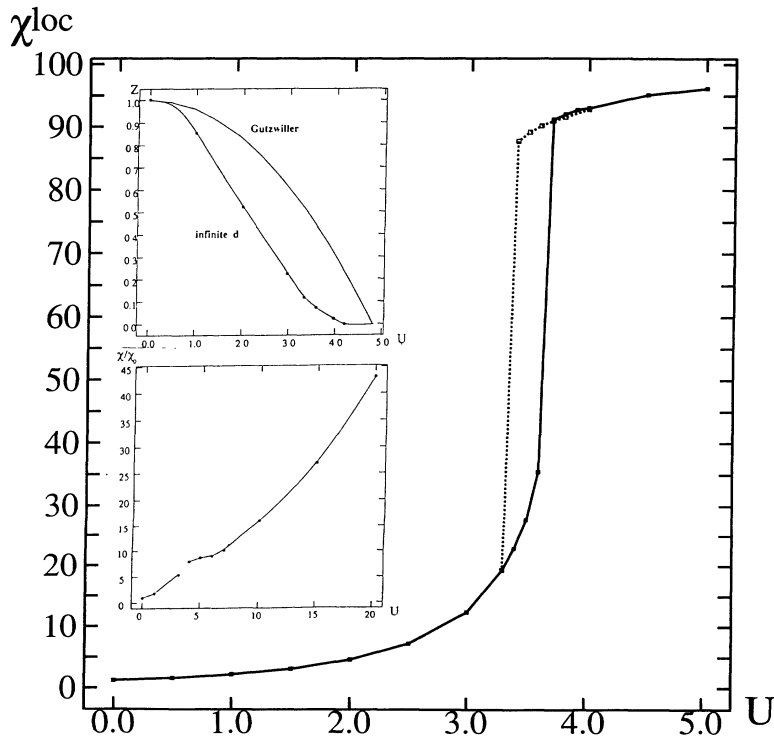


FIG. 1.  $\chi_{\text{loc}}$  vs  $U$  at zero field, for  $\beta t = 100$  ( $n_s = 5$ ). A coexistence region between  $U_{c1} = 3.3$  and  $U_{c2} = 3.8$  is clearly apparent. Top inset:  $Z$  vs  $U$ , numerical solution (dots and curve) (Ref. 26) and Gutzwiller approximation (full line). Bottom inset: uniform susceptibility  $\chi$  vs  $U$  for  $\beta = 100$  ( $n_s = 4$ ). Note the linear dependence for large  $U$ , with slope  $\sim 1/J = 2U/t^2$ .

ings in uniform and local quantities in this limit. This explains also why the  $d = \infty$  Mott insulating phase has a finite ground-state entropy  $N \ln 2$  but a finite uniform magnetic susceptibility ( $\chi = 1/J$  for large  $U$ ).

### III. OVERVIEW OF THE RESULTS FOR FINITE FIELD

Figure 2 displays our numerical results for the field dependence of the magnetization, for various values of  $U$  and a fixed temperature  $T = 0.01$ . Three different behaviors are clearly seen. For the smaller values of  $U$ , a unique metallic solution is found in which the magnetization smoothly saturates as the field is increased. For the larger values of  $U$ , a unique insulating solution is found in which the magnetization quickly saturates [corresponding to a large  $\chi(h = 0)$ ], and a rapid crossover from the Mott insulator to the fully polarized band insulator is found. The most interesting behavior arises for intermediate values of  $U$ , an example of which is  $U = 3$  on Fig. 2. There, two different solutions are found, one at lower field is “metallic” (for a more precise characterization, see Sec. V), and disappears at some critical field  $h_{c2}(U, T)$  and the other is “insulating” and only exists at fields larger than  $h_{c1}(U, T)$ . We find for  $U = 3$  and  $T = 0.01$  that a coexistence region exists, i.e., that  $h_{c1} \simeq 0.13 < h_{c2} \simeq 0.17$ . Note that the value  $U = 3$  is below the critical value  $U_{c1}(h = 0, T = 0.01)$  above which an insulating solution is found in zero field (this is why  $h_{c1} > 0$  in this case). Hence a magnetic field drives the strongly correlated metal to a first-order metal-insulator transition at some critical field at which the magneti-

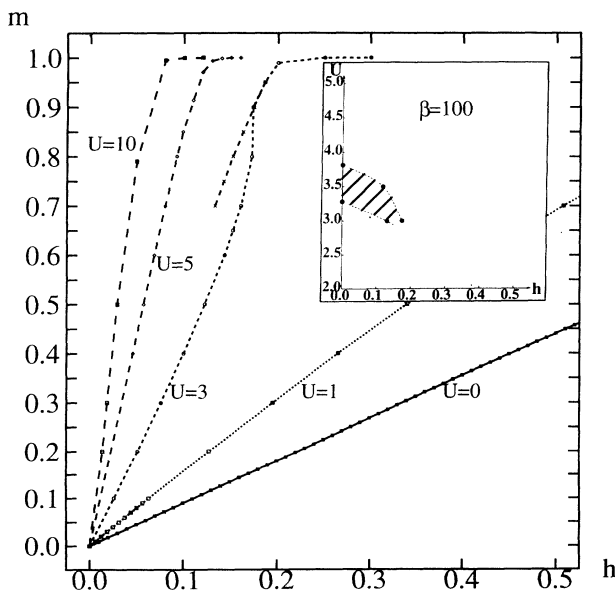


FIG. 2. Magnetization curves  $m(h)$  for, from below,  $U = 0, 1, 3, 5, 10$  ( $\beta t = 100$  and  $n_s = 4$ ). Note the three regimes: metallic at small  $U$  ( $U = 0, 1$ ), insulator at large  $U$  ( $U = 5, 10$ ), and the transition region ( $U = 3$ ). Inset: schematic phase diagram in the  $(U, h)$  plane for  $T=0.01$ .

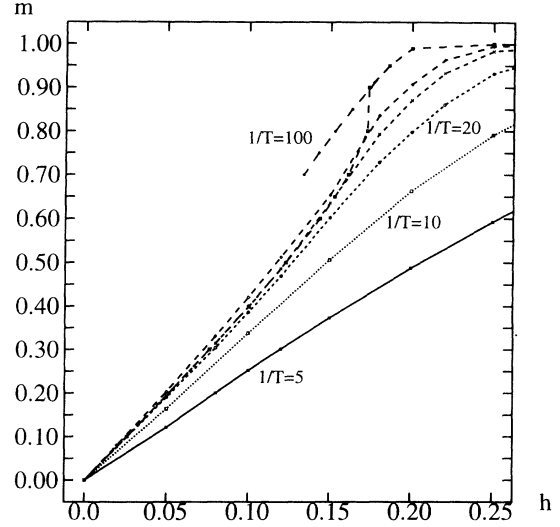


FIG. 3.  $m$  vs  $h$  for  $U = 3$ ,  $\beta = 5, 10, 20, 30, 40, 100$  (from below), and  $n_s = 4$ . The magnetic-field-induced phase transition occurs only at low temperature ( $\beta \geq 50$ ).

zation jumps discontinuously (metamagnetic transition). It plays, in this respect, a role similar to temperature, which also drives the Mott transition to become first order. We have also calculated magnetization curves for  $U = 3.5$ , which lies inside the zero-field coexistence region at  $T = 0.01$ , so that both a metallic and an insulating solution exist for small fields. Based on these findings, we can draw an estimate of the phase diagram in the  $(U, h)$  plane at  $T = 0.01$ , as shown in the inset of Fig. 2.

One can also follow the temperature dependence of these solutions, as shown in Fig. 3 for  $U = 3$ . It is only at the lowest temperatures studied that the coexistence sets in. For temperatures  $T$  above roughly  $1/50$  in this case, a single solution is recovered. For this reason, a detailed investigation of this phenomenon is beyond the reach of present Monte Carlo methods and has escaped previous studies.<sup>9,11,17</sup>

### IV. MAGNETIC PROPERTIES IN THE GUTZWILLER APPROXIMATION

For further comparison with our results, we review in this section some aspects of the response to a magnetic field of the Hubbard model within the Gutzwiller approximation. The Gutzwiller method<sup>1-4</sup> is a zero-temperature variational approach, which relies on the ground-state wave function:  $g^D |FS\rangle$ , where  $|FS\rangle$  denotes a free Fermi sea,  $D$  is the double occupancy operator  $D = \sum_i n_{i\uparrow} n_{i\downarrow}$ , and  $0 \leq g \leq 1$  is a variational parameter. In the limit of infinite dimensions, average values computed with this wave function coincide with the results of the “Gutzwiller approximation,” so that no distinction needs to be made between the two approaches.<sup>14</sup>

At half filling and for finite  $h$ , the variational ground-

state energy reads (using  $d \equiv \langle n_\uparrow n_\downarrow \rangle$  as a variational parameter instead of  $g$ ):

$$E_g = 4d \frac{1 - 2d + \sqrt{(1 - 2d)^2 - m^2}}{1 - m^2} \epsilon_0(m) + Ud, \quad (14)$$

where

$$\epsilon_0(m) = \int_{-\infty}^{\mu_0(n_\uparrow)} d\epsilon \epsilon D(\epsilon) + \int_{-\infty}^{\mu_0(n_\downarrow)} d\epsilon \epsilon D(\epsilon). \quad (15)$$

The corresponding applied field is obtained from  $h = \frac{\partial E_g}{\partial m}$ .

For zero external field, the solution of this variational problem predicts<sup>2</sup> a second-order Mott transition at the Brinkman-Rice point  $U_{BR} = \frac{32\sqrt{2}}{3\pi} \simeq 4.8$  between a metallic phase for  $U < U_{BR}$  and an insulating phase for  $U > U_{BR}$ . This transition is characterized by the divergence of the effective mass [ $Z = m/m^* = 1 - (U/U_{BR})^2$ ], the susceptibility ( $\chi/\chi_0 \propto m^*/m$ ) and the inverse of the compressibility. The gap of the insulating solution opens up continuously at  $U_{BR}$ :  $\Delta_g \propto (U - U_{BR})^{1/2}$ . Because the exchange is neglected in this description, the insulator is just a collection of independent local moments: the ground-state entropy is  $N \ln 2$ , and both the local and uniform magnetic susceptibility are infinite at zero temperature (in contrast to the  $d = \infty$  description which has  $\chi_{loc} = \infty$  but  $\chi$  finite). Finite-temperature extensions of the Gutzwiller approximation, following, e.g., the four-slab-boson scheme,<sup>6</sup> predict a first-order transition for  $T > 0$ .<sup>4</sup>

The effect of a uniform magnetic field  $h$  within the Gutzwiller approximation has been addressed in detail by Vollhardt<sup>3</sup> and by Nozières.<sup>4</sup> For small  $U$ , the magnetization of the metal smoothly saturates with  $\partial\chi/\partial h < 0$ . But, for  $U \geq 0.44U_{BR}$ , the metal becomes metamagnetic with  $\partial\chi/\partial h > 0$ . Furthermore, close enough to  $U_{BR}$ ,  $Z$  decreases upon increasing  $h$ : the field drives the system closer to localization. A general thermodynamical identity ("Maxwell relation") relates the specific-heat enhancement to the low-temperature behavior of the susceptibility:

$$\frac{\partial^2 \chi}{\partial T^2} = \frac{\partial^2 C_v / T}{\partial h^2} \equiv -\frac{2\pi^2}{3} D(0) \frac{1}{Z(h=0)^2} \frac{\partial^2 Z}{\partial h^2}, \quad (16)$$

where all derivatives are taken at  $h = T = 0$ . This implies<sup>4</sup> that any consistent finite-temperature extension of the Gutzwiller approximation would yield  $\partial\chi/\partial T > 0$  close to  $U_{BR}$ .

Furthermore, for sufficiently large  $U$ , the variational equations have three solutions in a certain range of values of  $h$ , one of which is unstable thermodynamically. A mixture of the two stable solutions may lower the energy, and a Maxwell construction must be made to find the field at which a first-order transition takes place.<sup>4</sup> The resulting magnetization curves  $m(h)$  are depicted in Fig. 4 for various values of  $U$ . Hence, a line of first-order phase transition is found in the plane  $(U, h)$ , as shown in the inset of Fig. 4, ending at a second-order point  $(U_c, h_c)$ . Correspondingly, a coexistence region can be

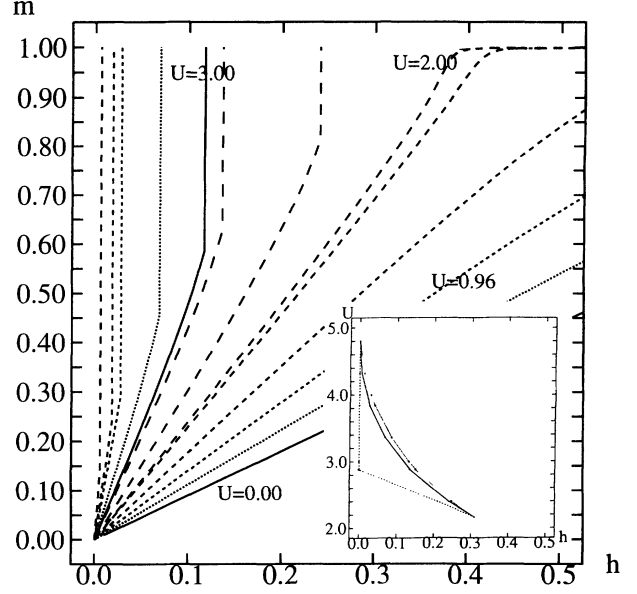


FIG. 4. Magnetization vs  $h$  in the Gutzwiller approximation for  $U/U_{BR} = 0, 0.1, 0.2, \dots, 0.9$  and also  $U = 2, 3, 4$  for comparison with Fig. 2. The Maxwell construction has been done for  $U > 0.44U_{BR}$ . Inset:  $(U, h)$  phase diagram at  $T = 0$  in the Gutzwiller approximation; phase coexistence region  $[U(h_{c1}), U(h_{c2})]$  (dotted lines), and first-order line (full curve) ending at second-order points  $(U_{BR}, h = 0)$  and  $(U_c, h_c)$ .

drawn in the  $(U, m)$  plane: phase separation takes place for  $m_{c1}(U) < m < m_{c2}(U)$  when  $U > U_c$ .

## V. RESULTS AND DISCUSSION

### A. The weakly correlated metal

We consider first the metallic phase with moderate correlation effects ( $U$  much smaller than  $U_{c1}$ ). There, the effect of a magnetic field is to drive the system from the unpolarized to the fully magnetized Fermi liquid, which at half filling is actually a band insulator. This process is a smooth crossover. Because of the Pauli principle, the polarization of the spins makes the interaction term  $n_\uparrow n_\downarrow$  less and less effective as the field is increased. Accordingly, the interaction-enhanced effective mass decreases smoothly towards  $m^* = m$  as  $h$  increases, as depicted in the inset of Fig. 5, where  $Z = m/m^*$  is plotted vs  $h$  for  $U = 1$ . The crossover scale is the effective Fermi energy or spin-fluctuation Kondo scale  $T_K$ . The Fermi-liquid (metallic) character of the solution all the way to the fully polarized state is demonstrated by checking that the solution always satisfies Luttinger theorem. In the presence of  $h$ , the latter reads:

$$\text{Re}\Sigma_\sigma(i0^+) - \mu = h\sigma - \mu_0(n_\sigma), \quad (17)$$

where  $\mu_0$  denotes the chemical potential of the noninteracting system. This condition expresses that the Fermi surface for each spin species accommodates exactly  $n_\sigma$  electrons.

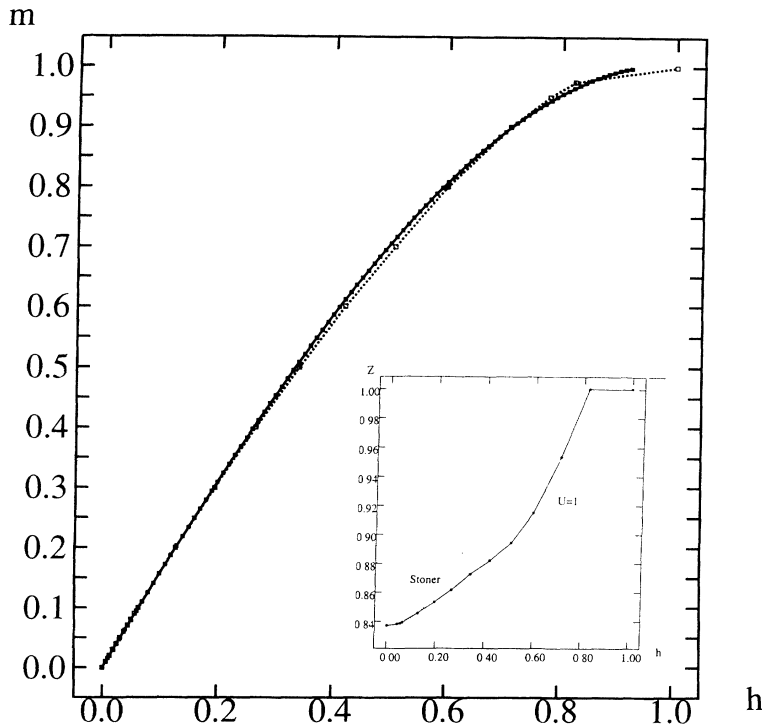


FIG. 5. Magnetization of the weakly correlated metal  $U = 1$  ( $\beta = 100$ ,  $n_s = 4$ ) (dashed curve). The Stoner prediction (full curve) obtained by adjusting the Stoner factor  $S = \chi/\chi_0$  is in excellent agreement with the infinite- $d$  result. Inset: Field-dependence of the quasiparticle residue  $Z(h)$  showing the crossover from the unpolarized to the fully polarized metal (band insulator). Low-field comparison to Eq. (20) (dashed curve).

In this regime of weak correlations, the Stoner approximation provides a good description of our results for  $m(h)$ . It is based on a Hartree-Fock decoupling of the interaction with respect to  $S_z$ , leading to the random-phase-approximation formula for the uniform susceptibility  $\chi/\chi_0 = [1 - \frac{U}{2}\chi_0]^{-1} = S$  ( $S$  is the so-called Stoner enhancement factor), and the magnetization is given, at  $T = 0$ , by

$$m_{\text{Stoner}} = 2 \int_0^{h - m_{\text{Stoner}} U/2} d\epsilon D(\epsilon). \quad (18)$$

This is compared to our results in Fig. 5, where the numerically obtained value of the ratio  $\chi(h=0)/\chi_0(h=0) \equiv S \simeq 1.74$  has been used as the input parameter of the fit. Within this approximation the low-temperature dependence of the susceptibility reads

$$\begin{aligned} \chi_{\text{Stoner}}(T)/\chi_0 &= S \left( 1 + \frac{\pi^2}{6} \frac{D''}{D} ST^2 + \dots \right) \\ &= S \left( 1 - \frac{\pi^2}{12} ST^2 + \dots \right), \end{aligned} \quad (19)$$

from which a low-field dependence of the quasiparticle residue can be inferred using Maxwell relation (16):

$$Z_{\text{Stoner}}(h) = Z(h=0) \left( 1 + \frac{h^2}{4} S^2 Z(h=0) + \dots \right). \quad (20)$$

This agrees very well with our results as shown on the inset of Fig. 5.

Since the physics at larger  $U$  is not that of a ferromagnetic instability ( $\chi$  remains finite), we have not at-

tempted to compare our results with partial resummations of spin-fluctuation diagrams beyond Hartree-Fock theory (as in the paramagnon approach<sup>20</sup>).

## B. The Mott insulator

As in the above case, the magnetization smoothly saturates for large  $U$  ( $\gg U_{c2}$ ) with  $\partial\chi/\partial h < 0$  (Fig. 6), but

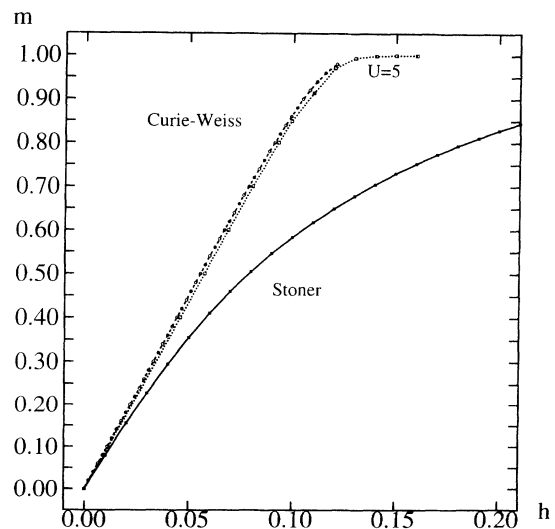


FIG. 6. Magnetization of the Mott insulator for  $U = 5$  ( $\beta = 100$ ,  $n_s = 4$ ) (small dashes with squares). A Stoner fit ( $S = \chi/\chi_0$ ) (lower curve) is very poor with saturation of the magnetization too slow. Conversely, a Curie-Weiss law with  $J = t^2/2U$  and  $U = 5$  (big dashes with circles), is in excellent agreement with the infinite- $d$  result.

the crossover between the Mott insulator and the band insulator is now governed by a different scale: the antiferromagnetic exchange  $J = t^2/2U$ . Because the scale involved in *uniform* magnetic properties is the magnetic exchange between one spin and a shell of  $z$  antiparallel nearest neighbors, this scale survives the  $z \rightarrow \infty$  limit. This scale is absent in the Gutzwiller approximation, which yields  $m(h) = 1$  for all  $h$  at  $T = 0$ .

The Mott insulator has  $\text{Re}\Sigma(\omega + i0^+) \simeq 1/\omega$  at  $h = 0$ , but  $h$  cuts off this divergence, and a finite slope at zero frequency is recovered for  $h \neq 0$ :

$$\text{Re}\Sigma(\omega + i0^+) = \Sigma(i0^+) + (1 - 1/\alpha)\omega + \dots$$

(see Fig. 7). This can be simply understood from the low-frequency limit of the self-consistency relation (3):

$$\text{Re}\Sigma_\sigma(\omega + i0^+) = \omega + \mu + h\sigma - \frac{t^2}{2}\text{Re}G_\sigma(\omega + i0^+) - \text{Re}G_\sigma^{-1}(\omega + i0^+) \quad (21)$$

with

$$\begin{aligned} \text{Re}G_\sigma(\omega + i0^+) &= - \int d\epsilon \frac{\rho_\sigma(\epsilon)}{\epsilon} - \omega \int d\epsilon \frac{\rho'_\sigma(\epsilon)}{\epsilon} + \dots \\ &\equiv \rho_1 + \omega\rho_2 + \dots \end{aligned} \quad (22)$$

Since, in presence of a finite field, the DOS  $\rho_\sigma(\omega)$  is not symmetric, the integral  $\rho_1$  does not vanish, leading to the linear slope of  $\text{Re}\Sigma(\omega + i0^+)$ , with  $1/\alpha = \rho_2/\rho_1^2 - \rho_1 t^2/2$ .  $\alpha$  is a convenient measure of the crossover between the Mott insulator at  $h = 0$  ( $\alpha = 0$ ) and the band insulator at large  $h$  ( $\alpha = 1$ ), and is depicted in the inset of Fig. 7. The insulating (non-Fermi-liquid) character of the solution all

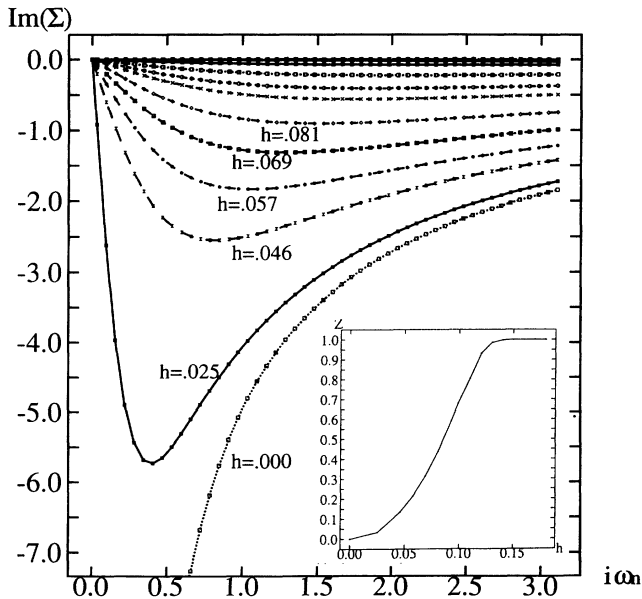


FIG. 7.  $\text{Im}\Sigma(i\omega_n)$  vs  $\omega$  at ( $U = 5$ ,  $\beta = 100$ , and  $n_s = 4$ ) for various values of  $h$  ( $0 < h < 0.2$ ). At  $h \neq 0$ , the divergence at  $\omega = 0$  is cut off, leading to a finite slope  $[1 - 1/\alpha(h)]$  at small frequencies. Inset: crossover from Mott insulator to band insulator (fully polarized) characterized by  $\alpha(h)$ .

the way from  $h = 0$  to saturation is evidenced by checking that the Luttinger theorem is violated.

As expected, the magnetization curves are very poorly described by a Stoner fit in this regime [adjusting the value of  $S$ , saturation is found at a much smaller field  $\simeq J$  in the actual results than in the Stoner curve (Fig. 6)]. A quantitative understanding of the results can nevertheless be reached by studying the large  $U$  limit of the fully connected model (5), along the lines of Ref. 11. For large  $U$  and at half filling, (5) reduces to a Hamiltonian for spin degrees of freedom, which reads

$$H = \sum_{ij} J_{ij} \mathbf{S}_i \cdot \mathbf{S}_j, \quad (23)$$

where  $J_{ij}$  are independent random variable with  $\overline{J_{ij}} = J/N$  and  $\overline{J_{ij}^2} - \overline{J_{ij}}^2 \propto J^2/N^2$ . Since the variance is of order  $1/N^2$  (not  $1/N$ ), the randomness becomes irrelevant in the thermodynamic limit. The partition function of the pure model is easily obtained by the steepest-descent method,<sup>11</sup> and the magnetization is simply given by the Weiss mean-field equation:

$$m = \tanh \beta[h - Jm] \quad \text{with} \quad J = \frac{t^2}{2U}. \quad (24)$$

The uniform susceptibility also reads simply<sup>11</sup>  $\chi(h = 0) = 1/(T + J)$ , while  $\chi_{\text{loc}} = 1/T$ .

Figure 6 shows the excellent agreement of expression (24) with the numerical results for  $U = 5$ . This emphasizes the dominant role of the exchange scale  $J$  in the Mott insulator, and the simplicity of its magnetic properties in the  $d = \infty$  limit.

Finally, the evolution of the local density of states  $\rho(\omega) = -\frac{1}{\pi}\text{Im}G(\omega + i0^+)$  obtained by exact diagonalization is consistent with the above scheme: as the field is increased, the gap is practically unaffected, but there is an asymmetric redistribution of spectral weight (controlled by  $J$ ) between the high-energy peaks corresponding to the upper Hubbard band.

### C. The Mott transition and the strongly correlated metal

We studied intensively the  $U = 3$  case both (i) at  $T = 0.01$  (by complete diagonalization with  $n_s = 4, 5, 6$ ) and (ii) at  $T = 0$  (by the Lanczòs method with  $n_s = 4, 6, 8$ ). We also studied the value  $U = 3.5$  which lies inside the zero-field coexistence region  $[U_{c1}, U_{c2}]$  at  $T = 0.01$ .

The central result is that two coexisting solutions are found in the interval  $h_{c1}(T) \leq h \leq h_{c2}(T)$  (see Fig. 8): one obtained by decreasing the field adiabatically from the saturated, high-field regime, and one obtained by increasing  $h$  adiabatically from the  $h = 0$  solution. An unambiguous way to discriminate between these solutions is to compare the value of  $\text{Re}\Sigma_\sigma(i0^+)$  for each of them with the one predicted by Luttinger theorem. This is done in the inset of Fig. 9 for the exact diagonalization results with  $n_s = 5$  at  $T = 0.01$ . Clearly, the solution obtained from the low-field one follows Luttinger theorem in all the

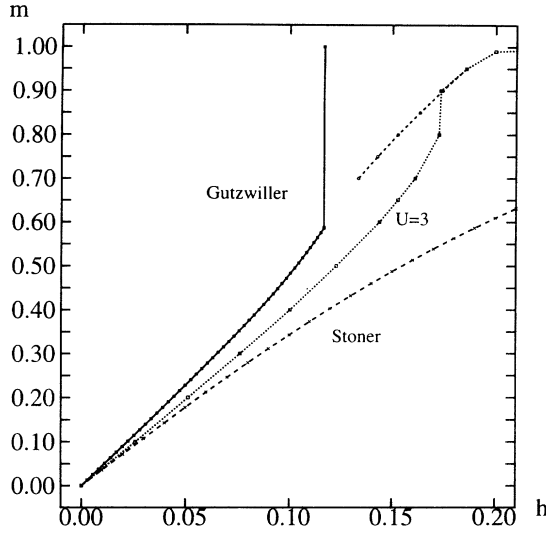


FIG. 8. Magnetization vs field at  $U = 3$  ( $\beta = 100$  and  $n_s = 5, 6$ ). Middle curve:  $d = \infty$  solution, exhibiting  $\partial m / \partial h > 0$ , and coexistence region (two solutions exist in the field interval  $0.13 < h < 0.17$ ). Stoner ( $S = \chi / \chi_0$ ) (lower) and Gutzwiller ( $U = 3$ ) (upper) curves for comparison.

region where it exists. On the contrary, the high-field one violates Luttinger theorem. Thus, two different phases are present: a metallic (Fermi-liquid) one obtained from the low-field regime and an insulating (non-Fermi-liquid) one obtained from the high-field regime.

For the finite temperature results ( $T = 0.01$ ,  $n_s = 4, 5$ ), the coexistence region  $[h_{c1}, h_{c2}]$  at  $U = 3$  is found

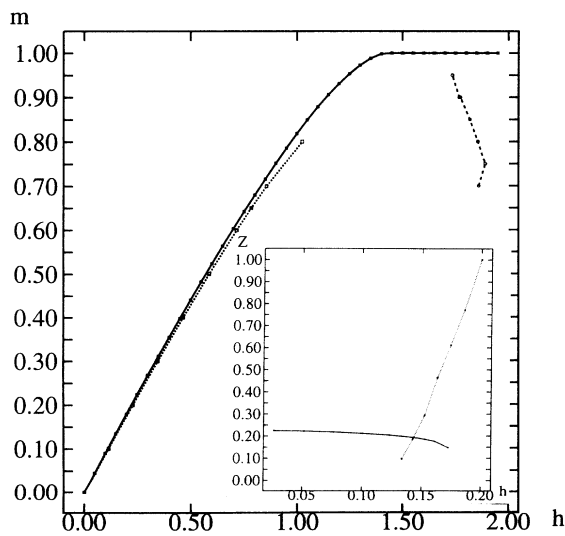


FIG. 9. Comparison of numerical solution with Luttinger theorem prediction:  $\text{Re}\Sigma_T(i0^+) - \mu = h - \mu_0(n_T)$ . The figure shows the two curves,  $m[h - \text{Re}\Sigma_T(i0^+) - \mu]$  (dashed line) and  $m[\mu_0(n_T)]$  (full line), which coincide when the Luttinger theorem is satisfied. The two curves differ for the insulating solution. Inset: Evolution of  $(1 - \partial\Sigma/\partial\omega)^{-1}$  vs  $h$  [ $Z(h)$  in the metal (full line),  $\alpha(h)$  in the insulator (dashed line)]. Note the small decreasing tendency of  $Z(h)$  on the metallic side close to the transition.

to be stabilized at the values  $h_{c1} \simeq 0.13, h_{c2} \simeq 0.17$  at  $U = 3$ . For  $U = 3.5$ ,  $h_{c1}$  is lowered to  $h_{c1} = 0$  as expected from the zero-field results. The situation is not so clear for the  $T = 0$  (Lanczòs) results: as noted in Ref. 28, a strong fluctuation of the field coexistence interval with the number of sites  $n_s$  is found.

Our results allow us to draw a rough estimate of the phase diagram in the  $(U, h)$  plane for a fixed low temperature (e.g.,  $T = 0.01$ ) (see inset of Fig. 2). A coexistence region  $[U_{c1}(h, T), U_{c2}(h, T)]$  is found, which becomes narrower with increasing field. The finite field, finite-temperature Mott transition is thus first order: the precise location of the transition requires a calculation of free energies (Maxwell construction), which has not been attempted in this work. The recent results of Ref. 12 suggests that the first-order transition “surface”  $U_c(h, T)$  ends at a second-order critical point at  $h = T = 0$ :  $U_c(h = 0, T = 0) = U_{c2}(h = 0, T = 0)$ . Thus, the qualitative features of the phase diagram are in rather good agreement with the predictions of the Gutzwiller approximation: the Mott transition is indeed lowered and driven to first-order when a magnetic field is applied.

Finally, we characterize the physical properties of the strongly correlated metal in a magnetic field (see Fig. 8). The magnetization curve  $m(h)$  starts linearly at  $U = 3$ , and it shows a metamagnetic curvature ( $\partial\chi/\partial h > 0$ ) close to the transition. This result has been obtained at  $\beta = 100$  and confirmed as a function of the number of sites of the exact diagonalization procedure.

In comparison, the Stoner prediction (with  $S$  fitted from the  $h = 0$  slope) has an appreciably larger downward curvature [faster saturation of  $m(h)$ ], while the Gutzwiller approximation yields too large an upward curvature (thus predicting a stronger metamagnetism at low field than what we find), and a first-order transition at a lower magnetic field than what we find. Similarly, the quasiparticle residue  $Z(h)$  at  $U = 3$  is practically constant in the metal with a small decreasing tendency (increase in  $m^*$ ) near the coexistence region (see Fig. 9). Again, the Gutzwiller approximation would predict too large an increase of the effective mass upon increasing the field at low field. However, most of the qualitative predictions of the Gutzwiller approximation are in good agreement with our results.

Here also, we have found it difficult to reliably estimate the low-temperature dependence of the zero-field susceptibility (i.e., the sign of the  $T^2$  correction). However, the trend of the complete diagonalization results with  $n_s = 4, 5, 6$  and the Lanczòs converged values are compatible with a very flat  $\chi(T)$ , consistent with the flatness of  $Z(h)$  and Maxwell identity (16).

Finally, the local density of states obtained in the coexistence region is consistent with the characteristics of the two phases: the metallic solution still has spectral weight at the Fermi level, while the other one displays a gap.

## VI. CONCLUDING REMARKS AND EXPERIMENTAL RELEVANCE

We have studied in this paper the effect of a uniform magnetic field on the paramagnetic solutions of the half-

filled Hubbard model in the limit of infinite dimensions. Depending on the interaction strength, three regimes can be identified (cf. Fig. 2).

In the weakly correlated metal at small  $U$ , the magnetic field reduces the effect of the interaction because of the Pauli principle. A smooth crossover is found between the unpolarized metal and the fully polarized band insulator, with a mass enhancement  $m^*/m$  decreasing smoothly to unity. The field dependence of the magnetization at zero temperature is reasonably described by the Stoner formula.

The uniform magnetic response of the Mott insulator at large  $U$  is controlled by the antiferromagnetic exchange  $J \simeq t^2/U$ , while the local susceptibility follows a Curie law. The field dependence of the magnetization is described very well by a simple Curie-Weiss mean-field expression.

The most interesting magnetic properties are found at intermediate values of  $U$ , close to the zero-field Mott transition. The applied magnetic field induces a first-order metamagnetic transition between the strongly correlated metal at low field and the high-field Mott insulator, forcing a jump in the magnetization curve. Similarly, the temperature drives first-order the zero-field metal-insulator transition. This is in qualitative agreement with the predictions of the Gutzwiller approximation. Quantitatively, however, this approximation does not describe our results very well because it neglects the magnetic exchange. For example, the critical field is predicted to be too low, and the upward curvature of the  $m(h)$  curve at low field much too large. Finally, we discuss the experimental relevance of the present study for the magnetic properties of transition metal oxides and liquid  $^3\text{He}$ .

Reference 18 reports measurements of the temperature dependence of the susceptibility for  $(\text{V}_{1-x}\text{Cr}_x)_2\text{O}_3$  for various Cr concentrations  $x$ . Sample 2 of this paper ( $x = 0.008$ ) displays two phase transitions as the temperature is raised: from an antiferromagnetic insulator to a paramagnetic metal (at  $T_N \simeq 175$  K), then from the metal to a paramagnetic Mott insulator (at  $T_{MI} \simeq 250$  K). The measured  $\chi(T)$  is reproduced in part in the inset of Fig. 10. Both transitions are clearly visible on this curve, even though the second one is much broadened for reasons explained in Ref. 18. The Mott transition is signaled by an increase of the susceptibility. Interestingly,  $\chi(T)$  decreases with temperature both in the metal and in the insulator above the transition region. Our treatment of the Hubbard model can account qualitatively for this behavior, as shown on Fig. 10 displaying the uniform susceptibility vs temperature found for  $U = 3.4$ . The metallic solution must be followed at low temperature, until the first-order transition to the Mott insulator is reached. Note that the temperature scale for the disappearance of the metal is considerably lowered as compared to a typical electronic scale of  $t \simeq 10^4$  K, and indeed falls in the range of  $10^2$  K. Quantitatively, however, the typical increase of  $\chi$  through the Mott transition is found to be larger than the experimental values even after correcting for the observed broadening.

Regarding liquid  $^3\text{He}$ , the main conclusion of our work

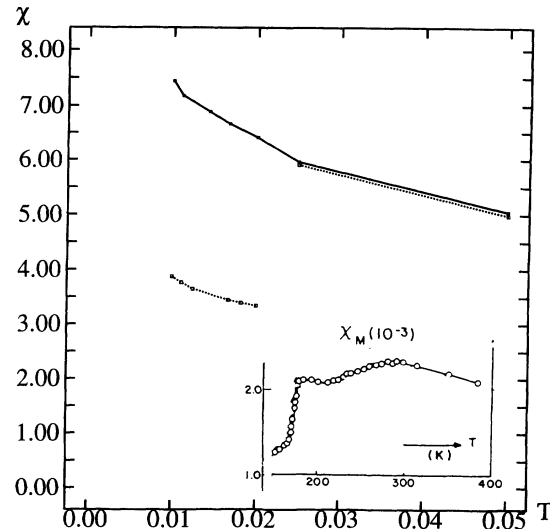


FIG. 10. Uniform susceptibility  $\chi$  vs temperature for  $U = 3.4$  (in the  $T = 0.01$  coexistence region) calculated with  $n_s = 4$ . Lower curve (dotted): metallic solution. Upper curve (full): insulating solution. A first-order metal-insulator transition between the two branches takes place upon heating. Inset: Results of Ref. 18 for  $(\text{V}_{1-x}\text{Cr}_x)_2\text{O}_3$  (sample 2,  $x = 0.008$ ). The first sharp rise corresponds to the Néel temperature, followed by the (rounded) metal-Mott insulator transition.

is that the metamagnetic transition of the half-filled Hubbard model is not an artefact of neglecting the exchange in the Gutzwiller approximation but is indeed present in the more refined  $d = \infty$  treatment. In spite of the fact that we would predict an appreciably larger critical field for this transition, our results for  $m(h)$  are hardly compatible with experiments.<sup>19</sup> This means that a lattice description of liquid  $^3\text{He}$  by a Hubbard model rigidly maintained at half filling is not satisfactory. Introducing vacancies,<sup>30</sup> while keeping  $U$  close to the half-filled Mott transition might avoid metamagnetism, but will still be faced with a much too small susceptibility enhancement, of order  $1/J$  (not  $1/T_K$ ) as soon as the exchange is correctly taken into account. A lattice description, if at all possible, must find a way of suppressing the exchange to restore the properties of a liquid (e.g., by working at very large  $U$  as a function of vacancy concentration).

#### ACKNOWLEDGMENTS

We acknowledge fruitful discussions with E. Wolf on the polarized  $^3\text{He}$  experiments and with M. T. Beal-Monod on paramagnon theory. We are grateful to M. Caffarel for a previous collaboration on the exact diagonalization algorithm and generous exchange of programs. This work was supported by DRET Contract No. 921479, and L. Laloux is supported by a 'Ministère de la Recherche et de l'Espace' contract. Laboratoire de Physique Théorique is Unité propre du CNRS (UP 701) associée à l'ENS et à l'Université Paris-Sud. Laboratoire de Physique Statistique is Laboratoire associé au CNRS (URA 1306) et aux Universités Paris VI et Paris.

- \* Electronic address: laloux@physique.ens.fr  
 † Electronic address: georges@physique.ens.fr  
 ‡ Electronic address: krauth@physique.ens.fr
- <sup>1</sup> M. C. Gutzwiller, *Phys. Rev.* **137**, A1726 (1965).
  - <sup>2</sup> W. F. Brinkman and T. M. Rice, *Phys. Rev. B* **2**, 4302 (1970).
  - <sup>3</sup> D. Vollhardt, *Rev. Mod. Phys.* **56**, 99 (1984).
  - <sup>4</sup> P. Nozières (unpublished).
  - <sup>5</sup> K. Seiler, C. Gros, T. M. Rice, K. Ueda, and D. Vollhardt, *J. Low Temp. Phys.* **64**, 195 (1986).
  - <sup>6</sup> G. Kotliar and A. Ruckenstein, *Phys. Rev. Lett.* **57**, 1362 (1986).
  - <sup>7</sup> A. Georges and W. Krauth, *Phys. Rev. Lett.* **69**, 1240 (1992).
  - <sup>8</sup> M. Rozenberg, X. Y. Zhang, and G. Kotliar, *Phys. Rev. Lett.* **69**, 1236 (1992).
  - <sup>9</sup> A. Georges and W. Krauth, *Phys. Rev. B* **48**, 7167 (1993).
  - <sup>10</sup> X. Y. Zhang, M. Rozenberg, and G. Kotliar, *Phys. Rev. Lett.* **70**, 1666 (1993).
  - <sup>11</sup> M. Rozenberg, G. Kotliar, and X. Y. Zhang, *Phys. Rev. B* **49**, 10 181 (1994).
  - <sup>12</sup> M. Rozenberg, G. Moeller, and G. Kotliar (unpublished).
  - <sup>13</sup> G. Moeller, Q. Si, G. Kotliar, and M. Rozenberg (unpublished).
  - <sup>14</sup> W. Metzner and D. Vollhardt, *Phys. Rev. Lett.* **62**, 324 (1989). For a recent review and references, see also D. Vollhardt, in *Correlated Electron Systems*, edited by V. Emery (World Scientific, Singapore, 1993).
  - <sup>15</sup> A. Georges and G. Kotliar, *Phys. Rev. B* **45**, 6479 (1992); A. Georges, G. Kotliar, and Q. Si, *Int. J. Mod. Phys. B* **6**, 705 (1992).
  - <sup>16</sup> M. Jarrell, *Phys. Rev. Lett.* **69**, 168 (1992).
  - <sup>17</sup> T. Saso and T. Hayashi (unpublished).
  - <sup>18</sup> A. Menth and J. P. Remeika, *Phys. Rev. B* **2**, 3756 (1970).
  - <sup>19</sup> S. Wieggers, P. E. Wolf, and L. Puech, *Phys. Rev. Lett.* **66**, 2895 (1991).
  - <sup>20</sup> For a review and references, see, e.g., K. Levin and O. T. Valls, *Phys. Rep.* **98**, 1 (1983); M. T. Beal-Monod, *Physica* **109-110B**, 1837 (1982).
  - <sup>21</sup> P. W. Anderson and W. F. Brinkman, *Phys. Rev. Lett.* **30**, 1108 (1973).
  - <sup>22</sup> U. Brandt and C. Mielsch, *Z. Phys. B* **75**, 365 (1989); **79**, 295 (1990); **82**, 37 (1991).
  - <sup>23</sup> V. Janis, *Z. Phys. B* **83**, 227 (1991).
  - <sup>24</sup> E. Muller-Hartmann, *Z. Phys. B* **74**, 507 (1989); **76**, 211 (1989).
  - <sup>25</sup> A. Georges and S. Sachdev (unpublished). The nonrandom limit of this fully connected model has been solved by P. van Dongen and D. Vollhardt, *Phys. Rev. B* **40**, 7252 (1989).
  - <sup>26</sup> M. Caffarel and W. Krauth, *Phys. Rev. Lett.* **72**, 1545 (1994).
  - <sup>27</sup> The fixed-magnetization algorithm is necessary, since more conventional modifications (e.g., attempts to break cycles) fail to yield convergence.
  - <sup>28</sup> B. Horvatic and V. Zlatic, *Solid State Commun.* **75**, 263 (1990).
  - <sup>29</sup> The constant  $U/2$  term is prescribed by the Luttinger theorem  $\Sigma(i0^+) = \mu = U/2$  (so that the zero-frequency spectral density sticks to the noninteracting value  $\rho(\omega = 0) = \sqrt{2}/\pi t$  for metallic solutions at  $h = 0$ ).
  - <sup>30</sup> D. Vollhardt, P. Wolfe, and P. W. Anderson, *Phys. Rev. B* **35**, 6703 (1987).